



# Growth rate affects blood flow rate to the tibia of the dinosaur *Maiasaura*

Roger S. Seymour<sup>1</sup> , Heath R. Caldwell<sup>2</sup>, Holly N. Woodward<sup>3</sup>  
and Qiaohui Hu<sup>1</sup> 

## Article

**Cite this article:** Seymour RS, Caldwell HR, Woodward HN, Hu Q (2024). Growth rate affects blood flow rate to the tibia of the dinosaur *Maiasaura*. *Paleobiology* **50**, 123–129. <https://doi.org/10.1017/pab.2023.24>

Received: 31 May 2023  
Accepted: 10 August 2023

**Corresponding author:**  
Roger S. Seymour;  
Email: [roger.seymour@adelaide.edu.au](mailto:roger.seymour@adelaide.edu.au)

<sup>1</sup>School of Biological Sciences, University of Adelaide, Adelaide, South Australia 5005, Australia;

E-mails: [roger.seymour@adelaide.edu.au](mailto:roger.seymour@adelaide.edu.au), [qiaohui.hu@adelaide.edu.au](mailto:qiaohui.hu@adelaide.edu.au)

<sup>2</sup>Department of Earth Sciences, Montana State University, Bozeman, Montana 59717, U.S.A.;

Email: [hebo6767@gmail.com](mailto:hebo6767@gmail.com)

<sup>3</sup>Oklahoma State University Center for Health Sciences, Tulsa, Oklahoma 74107, U.S.A.;

Email: [holly.ballard@okstate.edu](mailto:holly.ballard@okstate.edu)

### Non-technical Summary

Bones are living tissues and require oxygen from the blood circulation to grow, to replace damaged bone with new bone, and to carry out other functions. The amount of blood flowing into bones is related to the energy costs of these functions. It is difficult to measure blood flow rate into tissues, even in living animals, so it was thought impossible for it to be measured in extinct ones. However, blood enters the shaft of a leg bone through a hole, called a foramen, and the size of the foramen is related in turn to the size of its artery and the rate of blood flow. We can now use this surprisingly simple “foramen technique” to evaluate bone blood flow rates from fossil bones. In this study, we measured blood flow rate to the tibia (a lower hind-limb bone) of the dinosaur *Maiasaura* that lived more than 74 million years ago. They grew astonishingly fast, reaching 200–400 kg in their second year and reproductive adulthood in their third year and exceeding 3 metric tons before their teens. The fast growth of these hadrosaurs is associated with relatively high blood flow rates to the bones of juveniles compared with adults. Blood flow to 1 g of bone is 15 times higher in a 2 kg hatchling than in a full-grown adult, and that in a 1-year-old is 4 times higher. These differences reveal the enormous cost of building bones in the growth stages compared with the costs of maintaining them later in life.

### Abstract

Fossil bones were once living tissues that demanded internal blood perfusion in proportion to their metabolic requirements. Metabolic rates were primarily associated with bone growth (modeling) in the juvenile stages and with alteration and repair of existing bone affected by weight bearing and locomotion (remodeling) in later stages. This study estimates blood flow rates to the tibia shafts of the Late Cretaceous hadrosaurid *Maiasaura peeblesorum*, based on the size of the primary nutrient foramina in fossil bones. Foramen size quantitatively reflects arterial size and hence blood flow rate. The results showed that the bone metabolic intensity of juveniles (ca. 1 year old) was greater than fourfold higher than that of 6- to 11-year-old adults. This difference is much greater than expected from standard metabolic scaling and is interpreted as a shift from the high metabolic demands for primary bone modeling in the rapidly growing juveniles to a lower metabolic demand of adults to remodel their bones for repair of microfractures accumulated during locomotion and weight bearing. Large nutrient foramina of adults indicate a high level of cursorial locomotion characteristic of tachymetabolic endotherms. The practical value of these results is that juvenile and adult stages should be treated separately in interspecific analyses of bone perfusion in relation to body mass.

© The Author(s), 2023. Published by Cambridge University Press on behalf of The Paleontological Society. This is an Open Access article, distributed under the terms of the Creative Commons Attribution licence (<http://creativecommons.org/licenses/by/4.0/>), which permits unrestricted re-use, distribution and reproduction, provided the original article is properly cited.

**PALEOBIOLOGY**  
A PUBLICATION OF THE  
 PALEONTOLOGICAL SOCIETY

 **CAMBRIDGE**  
UNIVERSITY PRESS

## Introduction

Over the last half-century, evidence from fossil bones has been increasingly providing information on the physiological functions of archosaurs, especially the occurrence of endothermy (Benton 2021; Grigg et al. 2022). Part of the evidence for endothermy concerns rapid growth rates evident in bone histology. The burgeoning number of fossils has enabled the creation of growth curves of single taxa, for example, prosauropods (Chinsamy 1993), tyrannosaurs (Erickson et al. 2004; Carr 2020), ceratopsians (Erickson and Tumanova 2000), and hadrosaurs (Horner et al. 2000; Woodward et al. 2015). However, there have been no ontogenetic studies of bone metabolic physiology in any extinct dinosaur. The present study builds on a growth series of the hadrosaurid *Maiasaura peeblesorum* that revealed a rapid increase in body size with age (Woodward et al. 2015). Here, we investigate the blood perfusion rate of in the tibiae of this species to understand its role during development.



Bones are living tissues and therefore require a vascular circulation primarily to supply oxygen to aerobic cells within the bone tissues. The metabolic rate of bone cells is high (Schirmacher *et al.* 1997), and the interior of long bones is highly oxygenated (Bingmann and Wiemann 2007). Blood perfusion is particularly important during ontogeny, when the bones are rapidly growing and primary osteons are being laid down in a process known as bone modeling (Gilbert 1994). Mass-specific blood flow rates through long bones are higher in younger mammals than in older ones, which indicates higher bone metabolic demands (Pasternak *et al.* 1966; Whiteside *et al.* 1977; Nakano *et al.* 1986). After the animal reaches adulthood and its growth rate declines, the metabolic rates of bone cells become related to the costs of bone maintenance. In long bones, weight bearing and locomotion cause cortical microfractures due to static and dynamic stresses, and the damage needs to be repaired by replacing old bone with new bone in a process known as remodeling. Remodeling occurs by tiny capillary loops growing through old bone, accompanied on the front (the cutting cone) by osteoclasts that dissolve the damaged bone, followed by osteoblasts that deposit new bone in columnar secondary osteons (Robling *et al.* 2006; Doherty *et al.* 2015; Siddiqui and Partridge 2016). Increased intensity of locomotion results in a higher incidence of microfractures and an increase in remodeling (Lieberman *et al.* 2003; Eriksen 2010). Remodeling and fracture repair are associated with an increase in blood perfusion rate to the diaphysis of long bones (Tomlinson and Silva 2013; Stabley *et al.* 2014). In contrast, perfusion rate and the size of the principal nutrient artery decrease when weight bearing is reduced (Stabley *et al.* 2013).

Blood flow rates to supply adequate oxygen are much higher than would be required to supply nutrients and remove waste products, so the bone perfusion is matched to the oxygen requirements of bone metabolic rate (Ross *et al.* 1962). The metabolic rates demanded by tissues determine not only blood flow rates but also the size of the arteries delivering the blood (Seymour *et al.* 2019b). Where an artery passes through a foramen in bone, the size of the foramen is related to the size of the artery (Hu *et al.* 2021a). The vascular supply of long bones of mammals and birds includes three divisions: periosteal circulation to the surface of the bone, epiphyseal and metaphyseal supply to the ends of the bone, and the nutrient arteries to the shaft. The nutrient artery supplies 50–70% of the total bone perfusion in adult mammals (Trueta 1963). Therefore, measuring the size of the nutrient foramen can provide an indication of bone blood flow rate and hence an indication of bone metabolic rate. Flow rate was originally calculated from the foramen radius as the “blood flow index” ( $Q_i$ ) according to Hagen-Poiseuille principles (Seymour *et al.* 2012).

The foramen technique was initially applied to the femora of adult animals, because the role of bone shaft perfusion in adults was assumed to relate primarily to bone remodeling for repair of microfractures due to stresses and strains of locomotion. This assumption appeared reasonable, because  $Q_i$  in living mammals and birds increased with body mass with an exponent that was similar to the exponent for maximum metabolic rate of the animals running on treadmills (Seymour *et al.* 2012; Allan *et al.* 2014).

The original intention of the foramen technique was to apply it to extinct species for which foramina on fossil bones can be measured and compared with data from living species. It has been applied to the principal nutrient foramen on the shaft of long bones of fossil archosaurs (Seymour *et al.* 2012, 2019a), synapsids (Newham *et al.* 2020; Knaus *et al.* 2021), and plesiosaurs (Wintrich *et al.* 2019). Further research has been done on nutrient

foramina on the femora of extinct and living species of birds (Allan *et al.* 2014; Hu *et al.* 2023), including domestic chickens (Hu *et al.* 2020, 2021a,b).

In contrast to  $Q_i$  data from adult mammals that show a significant relationship with body mass (allometric exponent =  $0.86 \pm 0.11$  95% CI), the initial data from 10 species of Cretaceous dinosaurs were not significantly related to body size (exponent =  $0.24 \pm 0.47$ ) (Seymour *et al.* 2012). Furthermore, their  $Q_i$  data were higher than those of the mammals and revealed a great deal of variability. It is possible that some of the dinosaurs in our initial study were not fully grown and were exhibiting a greater perfusion rate required for bone growth. It is known that rapidly growing bones require enhanced perfusion to support their metabolic demands. The first study to use the foramen technique in a growth series concerned a diprotodont marsupial, the western grey kangaroo (*Macropus fuliginosus*) (Hu *et al.* 2018a,b). It revealed that  $Q_i$  of younger animals in the pouch greatly exceeded (by 50- to 100-fold) values from several adult species of diprotodont marsupials of the same body masses. Thus, growth (modeling) of young bones was confirmed to require a much higher blood flow rate, relative to bone volume, than does maintenance (remodeling) of the adult bone. The present study employs the foramen technique to evaluate the role of growth on long bone perfusion in a large, extinct dinosaur.

## Materials and Methods

Tibiae from the hadrosaur, *Maiasaura peeblesorum*, were examined in the Museum of the Rockies (MOR) in Bozeman, Montana, U.S.A. The 49 fossils were from the Two Medicine Formation (Campanian, Late Cretaceous), recovered from bonebeds discovered by John Horner and his field crews. Most of these fossils had been used in earlier studies involving thin sectioning for estimates of age and body mass (Woodward *et al.* 2015; Woodward 2019). All specimens were associated with accession numbers MOR 005 and MOR 758 only, but they had been given additional unique numbers (T1–T50). The tibiae were assumed to come from different individuals. Based on tibia length, there are two distinct size classes (eight at 362–485 mm and four at 780–930 mm).

Foramina were measured from photographs of the opening taken with a 12 MP digital camera. A nutrient foramen found on the femur of one hatchling *Maiasaura* (MOR 1002) was also measured with a Micro Cam USB Digital Camera. Photography was used so that alteration of the fossils was unnecessary. Photography is comparable to micro-CT scanning and impression molding if done with best practices and knowledge of foramen structure (Hu *et al.* 2020). A small scale with 1 mm increments was positioned in the same plane as the opening and as close to it as possible. Several setups were made, and photographs were compared to achieve the clearest measurement. Measuring was done on enlarged images with Fiji (Open Source, [www.fiji.sc](http://www.fiji.sc)), using the scale as reference. Midshaft circumference and total length of the entire fossil were measured to 1 mm with a flexible tape measure. The entire tibia was photographed against a larger scale, and the position of the nutrient foramen was indicated with an arrow.

The original paper on comparative foramen size calculated the blood flow index ( $Q_i$ ) from foramen radius and an arbitrary anatomical length (femur length) according to a simplified version of the textbook Hagen-Poiseuille equation for laminar flow in straight tubes (Seymour *et al.* 2012). Values of  $Q_i$  in units of

cubic millimeters had no direct meaning but were thought to be proportional to blood flow rate.  $Q_i$  remains useful for comparative purposes, but over the decade since its first use, we have made progress understanding its assumptions, finding some slightly inaccurate. We now know that actual blood flow rate ( $\dot{Q}$ ;  $\text{ml s}^{-1}$ ) in real arteries does not conform exactly to the theoretical Hagen-Poiseuille equation, which predicts that flow is proportional to arterial internal radius ( $r_i$ ; cm) raised to the constant power of 4 and inversely related to vessel length. Instead, a new theory predicts that the power changes depending on the radius (Huo and Kassab 2016). An empirical study based on 20 named arteries from nine species of mammals resulted a curved polynomial equation:  $\log \dot{Q} = -0.20 \log r_i^2 + 1.91 \log r_i + 1.82$  (Seymour et al. 2019b). This equation relies on vessel radius alone and does not require vessel length. We assume that a similar curve would apply to dinosaurs. Data from extant dinosaurs (birds) are too few to create a better equation; however, data from budgerigars fall in the 95% confidence limits of the mammalian equation (Schmaier et al. 2011). Another improvement is that we know that the lumen of a pressurized single nutrient artery in chickens occupies 20% of the foramen area and the veins and vessel walls occupy 80% (Hu et al. 2021a). Thus, we are now able to estimate nutrient artery  $\dot{Q}$  in meaningful units. In comparative studies,  $\dot{Q}$  produces less variation than  $Q_i$  calculated from the same foramina and is therefore considered superior (Hu et al. 2023).

Tibia volume ( $V_{\text{tib}}$ ;  $\text{cm}^3$ ) was calculated as the product of cross-sectional area at the minimum circumference and tibia length. This measure is not actual total bone volume, but is approximately proportional to it, considering that *Maiasaura* bones do not change shape much during growth (see Woodward et al. 2015: supplementary fig. 1).

Statistics involve least-squares linear regression on log-transformed data. All error statistics are 95% confidence intervals.

## Results

Measurable nutrient foramina were found on 13 tibiae. Putative foramina on 12 other specimens were not measured because they were unclear, overfilled, or occurred in an unusual place.

Definite nutrient foramina were located on the lateral side at  $35 \pm 2\%$  ( $n = 15$ ) of the total tibia length from the proximal end (Fig. 1A). No secondary foramina were discernible on the shafts. The nutrient vessels passed through the surface of the bone on an angle, and a vascular groove was often apparent on the proximal side of the foramen (Fig. 1B,E,F). Foramina were rarely unfilled (Fig. 1B), but usually contained contrasting sediment or artificial preparatory filler (Fig. 1E,F). Overfilled specimens were avoided, because the foramina usually flare at the surface, and the filler obscured the true dimensions of the canal. In one case of a broken tibia (T34), the foramen appeared in the middle of the cortical bone on the surface of the break (Fig. 1C).

The size of the nutrient foramen should ideally be measured by the cross-sectional area of the opening orthogonal to the direction of the tube axis. The dimensions of the foramen in a photograph depend on the position of the camera relative to the surface of the bone and the angle that the vessels pass through the bone surface. Therefore, we aimed the camera directly into the opening to produce as round an image as possible (Fig. 1B,F). In cases where material filled the opening below the flaring on the surface (Fig. 1E), the minor diameter was measured. Some minor diameters were measured from the width of the groove leading to the opening (Fig. 1B,F). For comparative purposes, we assumed that the foramen area was the same as that of a circle determined from minor diameter. This may have slightly underestimated the true area, but it was comparable in all specimens in this study and previous ones on fossil nutrient foramina (Seymour et al. 2012, 2019a).

Body mass ( $M_b$ ; kg) of the *Maiasaura* specimens was calculated from published tibia length ( $L$ , cm) according to the equation,  $M_b = 0.004L^{3.0}$  as regressed from data for eight specimens ranging in  $L$  from 56 to 93 cm (Woodward et al. 2015: supplementary table 2). The estimated age of the specimen at death was originally calculated by the relationship between age and body mass. Age was based on lines of arrested growth (LAGs) in five individual tibiae (Woodward et al. 2015: fig. 2B). However, the resultant von Bertalanffy equation asymptoted at a body mass (2337 kg) that was well below the estimated body

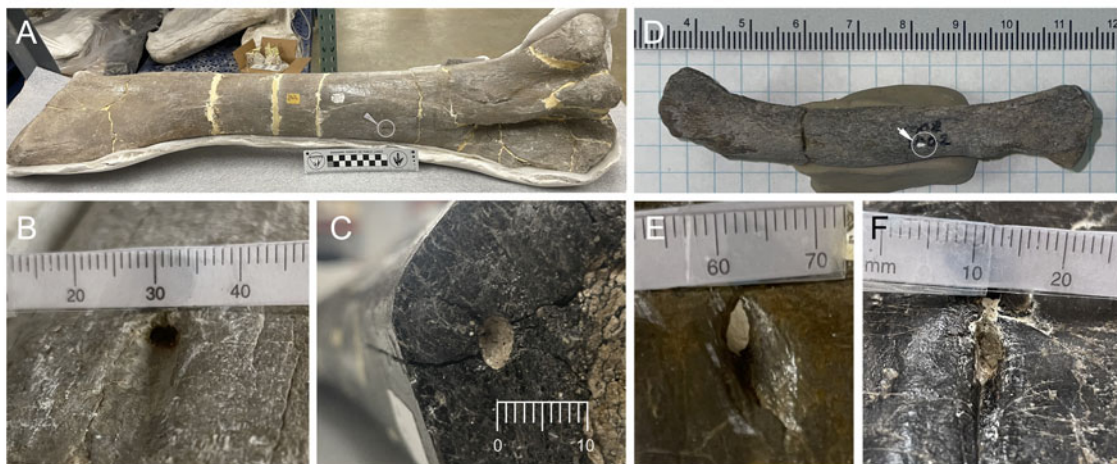


**Figure 1.** Principal nutrient foramina in the tibiae of *Maiasaura peeblesorum* in the Museum of the Rockies. A, Entire tibia of specimen T1 with the proximal end to the right and the foramen circled. B, Foramen of T1 looking along the groove into the opening. C, Broken end of the tibia of specimen T34 revealing the nutrient foramen in the middle of the black cortical bone and filled with sediment similar in color to that in the marrow cavity to the right. D, Femur of a hatchling specimen (MOR 1002) showing the circled nutrient foramen filled with talc for contrast. E, Foramen of T39 with sediment at the end of a deep groove. F, Foramen of T33 with sediment fill beyond its vascular groove. The specimens are all associated with the accession number MOR 005, except for the femur in D. All fine-scale units are millimeters.

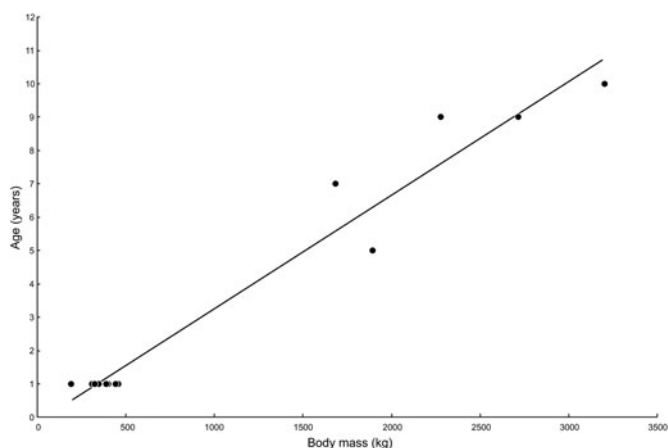


**Figure 2.** Relationship between estimated age ( $A$ ; years) and body mass ( $M_b$ ; kg) in *Maiasaura* during growth. Age was measured by the number of lines of arrested growth (LAGs) in histological cross sections of tibiae, and body mass was estimated from tibia length, according to Woodward *et al.* (2015). Tibiae without LAGs were considered to be 1 year old. The equation for the regression line is  $A = 0.0033 M_b - 0.1067$  ( $R^2 = 0.97$ ).

masses of several of the specimens we used. To solve this problem, we plotted LAG age on body mass for 13 specimens that provided clear foramen size in this study. Specimens without an internal LAG were taken as 1 year old (Horner *et al.* 2000, Woodward *et al.* 2015). A linear regression of age ( $A$ ; years) and  $M_b$  produced the equation,  $A = 0.0033 M_b - 0.1067$  ( $R^2 = 0.97$ ) (Fig. 2). This equation did not limit  $M_b$ , while corresponding well to LAG age, passing near the origin, and avoiding potential problems with inverse von Bertalanffy equations (Mackay and Moreau 1990).

Blood flow rates ( $\dot{Q}$ ) estimated from foramen size of young *Maiasaura* weighing 189–455 kg were similar to those of adults weighing 1680–3200 kg (Fig. 3). There was no significant difference in  $\dot{Q}$  between the group of eight smaller individuals ( $\dot{Q} = 6.27 \pm 1.17 \text{ ml min}^{-1}$ ) and the five larger ones ( $\dot{Q} = 10.00 \pm 5.44 \text{ ml min}^{-1}$ ) (*t*-test;  $p = 0.13$ ). The analysis included the foramen inside the bone cortex in specimen T34 (Fig. 1C), which appeared somewhat larger than the others that were

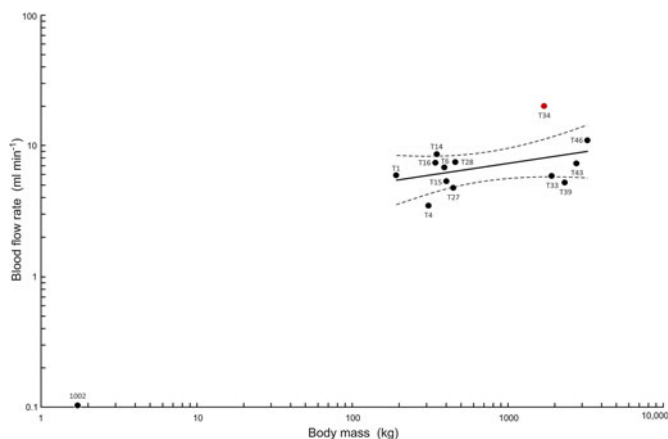


**Figure 3.** Blood flow rates ( $\text{ml min}^{-1}$ ) estimated from the minor radii of nutrient foramina in relation to body mass (kg) in *Maiasaura*, shown on logarithmic axes. Different tibiae are labeled according to the original study of Woodward *et al.* (2015), except for the point labeled 1002, which is from a femur of a 2 kg hatchling. The allometric equation ( $\dot{Q} = 2.15 M_b^{0.18}$ ) is based on 13 points, including T34, but not 1002. The 95% confidence bands for the regression mean are shown.

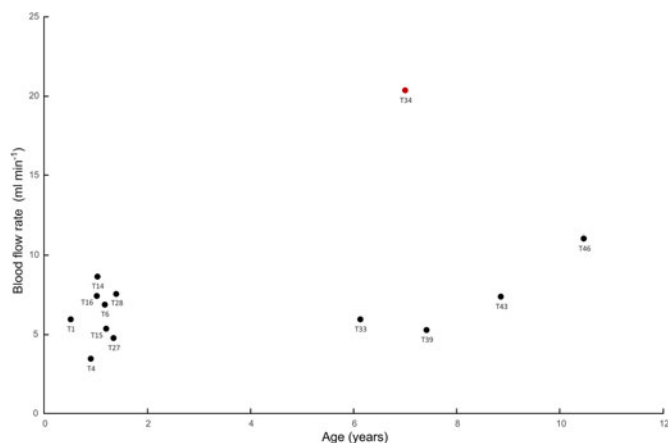


**Figure 4.** Blood flow rates ( $\text{ml min}^{-1}$ ) estimated from the minor radii of nutrient foramina in relation to age in *Maiasaura*. Age was calculated from body mass according to the regression equation in Fig. 2. Data labels as in Fig. 3.

photographed on the surface. Excluding the value from T34 resulted in  $\dot{Q} = 7.41 \pm 2.53 \text{ ml min}^{-1}$  in the four larger individuals. An allometric (power) equation set to all 13 points (i.e., including T34, not the femur of MOR 1002) yielded:  $\dot{Q} = 2.15 M_b^{0.18 \pm 0.26}$  ( $R^2 = 0.17$ ;  $p = 0.17$ ) (Fig. 3). The exponent is not significantly different from zero.

The smaller individuals were all about 1 year old, and the larger ones were estimated to be between 6 and 11 years old (Fig. 4). The same pattern was evident when  $\dot{Q}$  was plotted against the measure of tibia bone tissue volume ( $V_{\text{tib}}$ ;  $\text{cm}^3$ ) (Fig. 5). Blood flow rate on a bone volume-specific basis ( $\dot{Q}_{\text{vs}}$ ) indicated that the tibia bone tissue of young animals was much better perfused than that of older animals (Fig. 6).  $\dot{Q}_{\text{vs}}$  was significantly higher in the young group ( $0.0074 \pm 0.0015 \text{ ml min}^{-1} \text{ cm}^{-3}$ ) than in an older group ( $0.0017 \pm 0.0013 \text{ ml min}^{-1} \text{ cm}^{-3}$ ) (*t*-test;  $p < 0.001$ ). An allometric equation set to the 13 points yielded:  $\dot{Q}_{\text{vs}} = 1.88 V_{\text{tib}}^{-0.83 \pm 0.25}$  ( $R^2 = 0.82$ ;  $p < 0.0001$ ). The exponent is significantly less than zero and not significantly different from  $-1.0$ .

This study was limited by the fossil material available, so the distribution of ages is markedly uneven. Bone length ranged from 32.0 cm (T47) to 99.7 cm (T45) among the 49 available

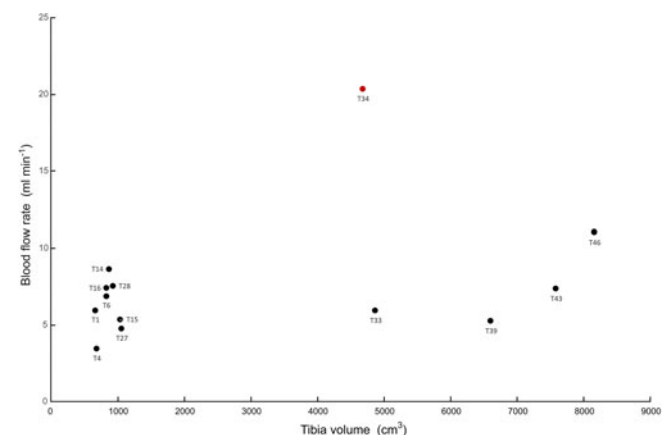


**Figure 5.** Blood flow rates ( $\text{ml min}^{-1}$ ) estimated from the minor radii of nutrient foramina in relation to values related to tibia volume ( $\text{cm}^3$  = midshaft cross-sectional area multiplied by bone length) in *Maiasaura*. Data labels as in Fig. 3.



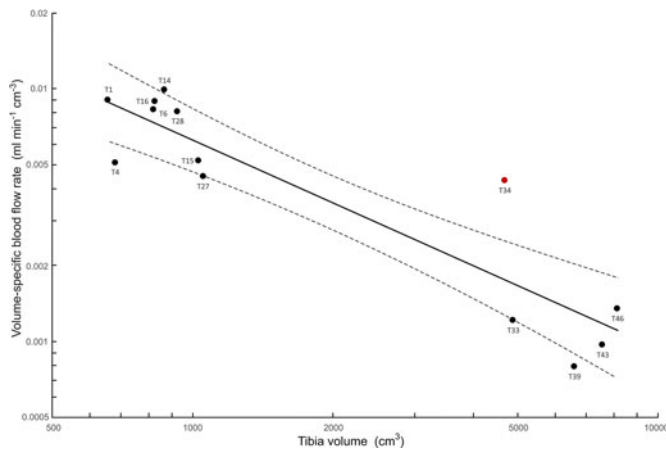


**Figure 6.** Bone volume-specific blood flow rates ( $\dot{Q}_{vs}$ ;  $\text{ml min}^{-1} \text{cm}^{-3}$ ) estimated from the minor radii of nutrient foramina in relation to values related to tibia volume ( $V_{tib}$ ;  $\text{cm}^3$  = midshaft cross-sectional area multiplied by bone length) in *Maiasaura*. The allometric equation ( $\dot{Q}_{vs} = 1.88 V_{tib}^{-0.83}$ ) is based on 13 points, including T34. The 95% confidence bands for the regression mean are shown. Data labels as in Fig. 3.

tibiae (Woodward et al. 2015: supplementary table 1). We found measurable foramina in specimens of a similar range in length from 36.2 cm (T8) to 93.0 cm (T46). Unfortunately, there were no tibiae from animals weighing less than approximately 189 kg. However, we found one femur from a very young *Maiasaura* (MOR 1002) (Fig. 1D). It was 7.55 cm long, with a midshaft circumference of 32 mm and an approximate volume ( $V$ ; see “Materials and Methods”) of  $6.15 \text{ cm}^3$ . Its size indicated an animal weighing about 2 kg. The nutrient foramen was 1.7 mm major diameter and 0.46 mm minor diameter. The minor foramen radius of 0.23 mm indicated a  $\dot{Q}$  of  $0.103 \text{ ml min}^{-1}$  (Fig. 3). If this fossil femur were a tibia, its  $\dot{Q}_{vs}$  value of  $0.0167 \text{ ml min}^{-1} \text{cm}^{-3}$  would be about twice those of the juveniles and 15 times higher than the adults.

## Discussion

This study supports the hypothesis that blood flow rate to bones is strongly influenced by high metabolic rates associated with bone growth in *Maiasaura*. The total blood flow rate does not increase significantly between 1-year-olds that are growing quickly to 6- to 11-year-olds that are reaching maximum body size (Fig. 3). Mean blood flow rate increases 1.6-fold, while mean body mass ( $M_b$ ) increases 6.6-fold and mean tibia volume ( $V_{tib}$ ) increases 7.9-fold. Thus, mean bone volume-specific blood flow rate ( $\dot{Q}_{vs}$ ) in the adults is only 23% of that of juveniles. By inference, the intensity of bone metabolic rate decreases markedly as the animals grow to adults.

Part of this decrease in bone blood flow might be expected, because the metabolic intensities of the tissues of animals tend to decrease with increasing  $M_b$  (so-called Kleiber’s law). The interspecific scaling exponents of whole-body metabolic rate in relation to  $M_b$  in adult birds and mammals is generally accepted to be between 0.67 and 0.75 (White et al. 2006). These exponents convert to mass-specific or volume-specific metabolic rate exponents of  $-0.33$  ( $= 0.67 - 1$ ) and  $-0.25$  ( $= 0.75 - 1$ ), respectively. The negative values indicate a decrease in specific metabolic rate with increasing  $M_b$ . This effect undoubtedly contributes to the decline in  $\dot{Q}_{vs}$  with  $V_{tib}$ , but the exponent for *Maiasaura* ( $-0.83 \pm 0.25$ ; Fig. 6) is significantly steeper than  $-0.33$  and

$-0.25$ . Taking the mass-specific exponent of  $-0.25$ , for example, a 6.6-fold increase in  $M_b$  (358 kg juvenile to 2353 kg adult) would result in a decrease of  $\dot{Q}_{vs}$  by a factor of 0.62 if standard metabolic scaling is assumed. Instead, the factorial decrease in  $\dot{Q}_{vs}$  is only 0.23, indicating that the juveniles had higher volume-specific bone perfusion rates than expected from standard metabolic scaling.

The interspecific analysis of whole-body metabolic rates of adult animals in the previous paragraph may in fact overestimate the effect of increasing body size during development in a single species. The exponents of metabolic rates during ontogeny vary widely among and within animal groups (Glazier 2005). For bird species, the exponents are higher during growth than in most interspecific studies of adults. For example, the exponents for whole-body metabolic rate on  $M_b$  are about 1.0 in broiler and Leghorn chickens over a 22- to 45-fold increase in  $M_b$  (Kuenzel and Kuenzel 1977), 0.77–0.87 in broiler chickens over a 12.6-fold growth in  $M_b$  (Tickle et al. 2018), and in the range of 0.99–1.09 in four species of wild fulmarine petrels over an approximately 10-fold change in  $M_b$  (Hodum and Weathers 2003). These scaling exponents close to 1 indicate that whole-body metabolic rate is proportional to  $M_b$ , so mass-specific rates are practically constant at all body masses during growth. Therefore, the steep decrease in bone  $\dot{Q}_{vs}$  with  $V_{tib}$  in *Maiasaura* is even more difficult to explain by whole-body effects. The explanation must lie specifically in bone physiology.

The results from this study are consistent with an ontogenetic study of long bone perfusion in the western grey kangaroo (*Macropus fuliginosus*), in which the foramen technique was used (Hu et al. 2018a,b). Blood flow rate was evaluated by calculating  $Q_i$  from foramen size. The new-born joey grows from birth at about 5 g to about 3 kg within the pouch and up to about 70 kg after leaving the pouch.  $Q_i$  increased with a steep exponent of 0.96 while in the pouch and shifted to a negative exponent of  $-0.59$  after the joey leaves the pouch and grows to adulthood. The markedly negative exponent in the latter phase is similar to the picture in *Maiasaura*, especially as this phase represents body masses growing through approximately one order of magnitude to the adult size in both the kangaroo and dinosaur. We suggest that there is a similar transition from growth (bone modeling) to maintenance (remodeling) during this phase in the mammal and the dinosaur.

Foramen sizes in adult *Maiasaura* tibiae are indicative of a high level of locomotory activity characteristic of a tachymetabolic, endothermic vertebrate. The foramen technique was first used to compare nutrient foramen size in the femora of a few species of dinosaur, including an unnamed hadrosaur, with those of extant mammals and reptiles (Seymour et al. 2012). It showed that perfusion rate, measured with femoral  $Q_i$ , was higher in the dinosaurs than in extant endothermic mammals, ectothermic varanids, and non-varanid reptiles. The present study is not directly comparable to the earlier one, because it measures  $\dot{Q}$  (not  $Q_i$ ) derived from tibiae (not femora). However, we can calculate  $Q_i$  and tibia volume from *Maiasaura* adults of the present study and compare them with  $Q_i$  values for mammals in relation to femur volume (see Seymour et al. 2012: supplementary fig. S3).  $Q_i$  data from the adult *Maiasaura* straddle the curve, demonstrating that large nutrient foramina indicate high bone perfusion rates in *Maiasaura*, consistent with mammalian-grade endothermy. Furthermore, hadrosaurs in general satisfy four other proxies for endothermy, including evidence from osteohistology (Horner et al. 2000; Woodward et al. 2015), evidence involving

endothermic levels of arterial blood pressure (Seymour 1976, 2016), evidence from the biomechanics of bipedality (Pontzer *et al.* 2009), and evidence from paleothermometry (Barrick *et al.* 1996; Dawson *et al.* 2020).

The results of this study are useful to interpret the use of the foramen technique in future studies of fossil bones. In comparative studies of extinct species, the juveniles should be removed, lest their apparently high perfusion rates be confused with the requirements for bone maintenance. Inclusion of juvenile specimens may have resulted in elevation of  $Q_i$  in the small, unidentified dinosaur species of our first foramen study (Seymour *et al.* 2012).

### Critique of Methods and Results

Working with fossil material is not ideal because of taphonomic alterations of the bone surface. We assume that the dimensions of the foramen are the same on a smooth fossil as on the original bone. However, fractures can obscure foramina in some cases and can create indentations that can be confused with foramina in others. Indents associated with longer fractures are rejected. Foramina can be filled with sediment or preparation material that is flush with the bone surface, therefore outlining the flared opening of the foramen, not the narrower canal. Such specimens are unacceptable for photography unless cleared of this material. However, the foramina in *Maiasaura* usually have a groove that accommodated the blood vessels leading to the opening (Fig. 1B,F). The width of this groove is the same size as the deeper foramen opening, so it can be measured even if the foramen is overfilled. This is best accomplished if the camera angle is aligned along the length of the groove (Fig. 1F).

The chance discovery of a cross section of an apparent nutrient foramen in specimen T34 (Fig. 1C) raises questions about the form of the foramen as it passes through the cortical bone. The section reveals an elliptical shape with a minor diameter of 3.75 mm, which is well above the mean and confidence interval of the other four adult specimens measured on the bone surface ( $2.42 \pm 0.33$  mm). Unfortunately, the periosteal surface opening is missing in T34, so there are at least four possible explanations for this difference. (1) The opening evident in T34 may not be a nutrient foramen. However, pneumatic foramina in dinosaurs occur in the axial and appendicular girdles, but not in the long bones (O'Connor 2006; Sereno *et al.* 2008; Benson *et al.* 2012), so we conclude that it is a nutrient foramen. (2) The foramen canal enlarges significantly deeper in the bone. Nutrient foramina typically contain both the nutrient artery and a larger vein. The cross sections of these can be round, elliptical or pear-shaped, but they do not change dimensions much in the middle of the cortical bone and widen only on the periosteal and endosteal surfaces (Hu *et al.* 2020, 2021a). Therefore, we reject midcortical widening as an explanation. (3) The foramen may be large because it services a larger tibia or because it comes from a reproductively active female that required an augmented rate of calcium mobilization for eggshell production. However, the volume of the tibia from T34 is equal to the smallest of the adult specimens (Fig. 5), so servicing more bone tissue is not the explanation. Femur perfusion rate in laying chicken hens is approximately twice that in non-laying hens, when measured by microsphere infusion (Hu *et al.* 2021b), and the lumen of the nutrient artery is larger in laying hens, indicating slightly greater flow (Hu *et al.* 2021a). However, these differences are not reflected in significant differences in foramen size in chickens, apparently because of high data variability. Thus, foramen size cannot

reliably determine differences in gender. (4) The most variation in foramen size appears between individuals of a species. In particular, the largest effective radius of the foramen is 1.8–2.0 times that of the smallest among 15 chickens (Hu *et al.* 2021a). Coincidentally, the ratio is 1.8 between the largest (T34) and smallest (T39) foramina in adult *Maiasaura*. We therefore consider that the foramen of T34 exhibits natural variation and is comparable to those of the others, which is why we included it in the analysis.

### Conclusions

Blood flow rates to the shafts of *Maiasaura* tibiae were estimated from the size of nutrient foramina in fossil bones. Because bone perfusion is related to bone metabolic rate, the relatively higher flow rates in juveniles can be explained by their higher oxygen demand for bone growth (modeling). Bone growth rate and relative blood flow rate decrease as the dinosaurs mature into adulthood, when bone perfusion becomes largely determined by maintenance and repair of bone tissue damaged by weight-bearing and locomotion (remodeling).

**Acknowledgments.** This project was supported by the Australian Research Council (grant no. DP 170104952) to R.S.S. The authors greatly appreciate the cooperation and assistance shown by the team at the Museum of the Rockies, in particular J. Scannella and E. Metz. J. Cubo, G. Grigg and one anonymous referee provided valuable comments on draft manuscripts.

**Competing Interests.** The authors declare no competing interests.

### Literature Cited

- Allan, G. H., P. Cassey, E. P. Snelling, S. K. Maloney, and R. S. Seymour. 2014. Blood flow for bone remodelling correlates with locomotion in living and extinct birds. *Journal of Experimental Biology* 217:2956–2962.
- Barrick, R. E., W. J. Showers, and A. G. Fischer. 1996. Comparison of thermoregulation of four ornithischian dinosaurs and a varanid lizard from the Cretaceous Two Medicine Formation: evidence from oxygen isotopes. *Palaio* 11:295–305.
- Benson, R. B. J., R. J. Butler, M. T. Carrano, and P. M. O'Connor. 2012. Air-filled postcranial bones in theropod dinosaurs: physiological implications and the “reptile”–bird transition. *Biological Reviews* 87:168–193.
- Benton, M. J. 2021. The origin of endothermy in synapsids and archosaurs and arms races in the Triassic. *Gondwana Research* 100:261–289.
- Bingmann, D., and M. Wiemann. 2007. O<sub>2</sub>-consumption, blood flow and PO<sub>2</sub> in bone. *Materialwissenschaft und Werkstofftechnik* 38:950–954.
- Carr, T. D. 2020. A high-resolution growth series of *Tyrannosaurus rex* obtained from multiple lines of evidence. *PeerJ* 8:e9192.
- Chinsamy, A. 1993. Bone histology and growth trajectory of the prosauropod dinosaur *Massospondylus carinatus* Owen. *Modern Geology* 18:319–329.
- Dawson, R. R., D. J. Field, P. M. Hull, D. K. Zelenitsky, F. Therrien, and H. P. Affek. 2020. Eggshell geochemistry reveals ancestral metabolic thermoregulation in Dinosauria. *Science Advances* 6:eaa9361.
- Doherty, A. H., C. K. Ghalambor, and S. W. Donahue. 2015. Evolutionary physiology of bone: bone metabolism in changing environments. *Physiology* 30:17–29.
- Erickson, G. M., and T. A. Tumanova. 2000. Growth curve of *Psittacosaurus mongoliensis* Osborn (Ceratopsia: Psittacosauridae) inferred from long bone histology. *Zoological Journal of the Linnean Society* 130:551–566.
- Erickson, G. M., P. J. Makovicky, P. J. Currie, M. A. Norell, S. A. Yerby, and C. A. Brochu. 2004. Gigantism and comparative life-history parameters of tyrannosaurid dinosaurs. *Nature* 430:772–775.
- Eriksen, E. F. 2010. Cellular mechanisms of bone remodelling. *Reviews in Endocrine and Metabolic Disorders* 11:219–227.

- Gilbert, S. F. 1994. Osteogenesis: the development of bones. Pp. 333–338 in S. F. Gilbert, ed. *Developmental biology*. 4<sup>th</sup> ed. Sinauer Associates, Sunderland, Mass.
- Glazier, D. S. 2005. Beyond the “3/4-power law”: variation in the intra- and inter-specific scaling of metabolic rate in animals. *Biological Reviews* 80:611–662.
- Grigg, G., J. Nowack, J. E. P. W. Bicudo, N. C. Bal, H. N. Woodward, and R. S. Seymour. 2022. Whole-body endothermy: ancient, homologous and widespread among the ancestors of mammals, birds and crocodylians. *Biological Reviews* 97:766–801.
- Hodum, P. J., and W. W. Weathers. 2003. Energetics of nestling growth and parental effort in Antarctic fulmarine petrels. *Journal of Experimental Biology* 206:2125–2133.
- Horner, J. R., A. De Ricqles, and K. Padian. 2000. Long bone histology of the hadrosaurid dinosaur *Maiasaura peeblesorum*: growth dynamics and physiology based on an ontogenetic series of skeletal elements. *Journal of Vertebrate Paleontology* 20:115–129.
- Hu, Q., T. J. Nelson, and R. S. Seymour. 2020. Bone foramen dimensions and blood flow calculation: best practices. *Journal of Anatomy* 236:357–369.
- Hu, Q., T. J. Nelson, and R. S. Seymour. 2021a. Morphology of the nutrient artery and its foramen in relation to femoral bone perfusion rates of laying and non-laying hens. *Journal of Anatomy* 240:94–106.
- Hu, Q., T. J. Nelson, and R. S. Seymour. 2021b. Regional femoral bone blood flow rates in laying and non-laying chickens estimated with fluorescent microspheres. *Journal of Experimental Biology* 224:jeb242597.
- Hu, Q., C. V. Miller, E. P. Snelling, and R. S. Seymour. 2023. Blood flow rates to leg bones of extinct birds indicate high levels of cursorial locomotion. *Paleobiology*. doi: <https://doi.org/10.1017/pab.2023.14>.
- Hu, Q. H., T. J. Nelson, E. P. Snelling, and R. S. Seymour. 2018a. Femoral bone perfusion through the nutrient foramen during growth and locomotor development of western grey kangaroos (*Macropus fuliginosus*). *Journal of Experimental Biology* 221:jeb168625.
- Hu, Q. H., T. J. Nelson, E. P. Snelling, and R. S. Seymour. 2018b. Correction: Femoral bone perfusion through the nutrient foramen during growth and locomotor development of western grey kangaroos (*Macropus fuliginosus*). *Journal of Experimental Biology* 221:jeb188029.
- Huo, Y. L., and G. S. Kassab. 2016. Scaling laws of coronary circulation in health and disease. *Journal of Biomechanics* 49:2531–2539.
- Knaus, P. L., A. H. Van Heteren, J. K. Lungmus, and P. M. Sander. 2021. Higher blood flow into the femur indicates elevated aerobic capacity in synapsids since the reptile-mammal split. *Frontiers in Ecology and Evolution* 2021:751238.
- Kuenzel, W. J., and N. T. Kuenzel. 1977. Basal metabolic rate in growing chicks *Gallus domesticus*. *Poultry Science* 56:619–627.
- Lieberman, D. E., O. M. Pearson, J. D. Polk, B. Demes, and A. W. Crompton. 2003. Optimization of bone growth and remodeling in response to loading in tapered mammalian limbs. *Journal of Experimental Biology* 206:3125–3128.
- Mackay, D., and J. Moreau. 1990. A note on the inverse function of the von Bertalanffy growth function. *Fishbyte* 8:28–31.
- Nakano, T., J. R. Thompson, R. J. Christopherson, and F. X. Aherne. 1986. Blood flow distribution in hind limb bones and joint cartilage from young growing pigs. *Canadian Journal of Veterinary Research* 50:96–100.
- Newham, E., P. G. Gill, P. Brewer, M. J. Benton, V. Fernandez, N. J. Gostling, D. Haberthür, et al. 2020. Reptile-like physiology in Early Jurassic stem-mammals. *Nature Communications* 11:5121.
- O'Connor, P. M. 2006. Postcranial pneumaticity: an evaluation of soft-tissue influences on the postcranial skeleton and the reconstruction of pulmonary anatomy in archosaurs. *Journal of Morphology* 267:1199–1226.
- Pasternak, H. S., P. J. Kelly, and C. A. Owen Jr. 1966. Estimation of oxygen consumption, and carbon dioxide production and blood flow of bone in growing and mature dogs. *Mayo Clinic Proceedings* 41:831–835.
- Pontzer, H., V. Allen, and J. R. Hutchinson. 2009. Biomechanics of running indicates endothermy in bipedal dinosaurs. *PLoS ONE* 4:127–135.
- Robling, A. G., A. B. Castillo, and C. H. Turner. 2006. Biomechanical and molecular regulation of bone remodeling. *Annual Review of Biomedical Engineering* 8:455–498.
- Ross, J. M., A. C. Guyton, H. M. Fairchild, and J. Weldy. 1962. Autoregulation of blood flow by oxygen lack. *American Journal of Physiology* 202:21–24.
- Schirrmacher, K., S. Lauterbach, and D. Bingmann. 1997. Oxygen consumption of calvarial bone cells *in vitro*. *Journal of Orthopaedic Research* 15:558–562.
- Schmaier, A. A., T. J. Stalker, J. J. Runge, D. Lee, C. Nagaswami, P. Mericko, M. Chen, S. Cliché, C. Gariépy, and L. F. Brass. 2011. Occlusive thrombi arise in mammals but not birds in response to arterial injury: evolutionary insight into human cardiovascular disease. *Blood* 118:3661–3669.
- Sereno, P. C., R. N. Martinez, J. A. Wilson, D. J. Varricchio, O. A. Alcober, and H. C. E. Larsson. 2008. Evidence for avian intrathoracic air sacs in a new predatory dinosaur from Argentina. *PLoS ONE* 3:e3303.
- Seymour, R. S. 1976. Dinosaurs, endothermy and blood pressure. *Nature* 262:207–208.
- Seymour, R. S. 2016. Cardiovascular physiology of dinosaurs. *Physiology* 31:430–441.
- Seymour, R. S., S. L. Smith, C. R. White, D. M. Henderson, and D. Schwarz-Wings. 2012. Blood flow to long bones indicates activity metabolism in mammals, reptiles and dinosaurs. *Proceedings of the Royal Society of London B* 279:451–456.
- Seymour, R. S., M. Ezcurra, D. Henderson, M. E. Jones, S. C. Maidment, C. V. Miller, S. J. Nesbitt, D. Schwarz, C. Sullivan, and E. Wilberg. 2019a. Large nutrient foramina in fossil femora indicate intense locomotor and metabolic activity in Triassic archosauromorphs and the pseudosuchian lineage. Society of Vertebrate Paleontology, 79th annual meeting, Abstracts of papers. Brisbane, QLD, Australia, p. 190.
- Seymour, R. S., Q. Hu, E. P. Snelling, and C. R. White. 2019b. Interspecific scaling of blood flow rates and arterial sizes in mammals. *Journal of Experimental Biology* 222:jeb 199554.
- Siddiqui, J. A., and N. C. Partridge. 2016. Physiological bone remodeling: systemic regulation and growth factor involvement. *Physiology* 31:233–245.
- Stabley, J. N., R. D. Prisby, B. J. Behnke, and M. D. Delp. 2013. Chronic skeletal unloading of the rat femur: mechanisms and functional consequences of vascular remodeling. *Bone* 57:355–360.
- Stabley, J. N., N. C. Moninga, B. J. Behnke, and M. D. Delp. 2014. Exercise training augments regional bone and marrow blood flow during exercise. *Medicine and Science in Sports and Exercise* 46:2107–2112.
- Tickle, P. G., J. R. Hutchinson, and J. R. Codd. 2018. Energy allocation and behaviour in the growing broiler chicken. *Scientific Reports* 8:4562.
- Tomlinson, R. E., and M. J. Silva. 2013. Skeletal blood flow in bone repair and maintenance. *Bone Research* 4:311–322.
- Trueta, J. 1963. The role of the vessels in osteogenesis. *Journal of Bone and Joint Surgery* 45:402–418.
- White, C. R., N. F. Phillips, and R. S. Seymour. 2006. The scaling and temperature dependence of vertebrate metabolism. *Biology Letters* 2:125–127.
- Whiteside, L. A., D. J. Simmons, and P. A. Lesker. 1977. Comparison of regional bone blood flow in areas with differing osteoblastic activity in the rabbit tibia. *Clinical Orthopaedics* 124:267–270.
- Wintrich, T., C. Fleischle, and P. M. Sander. 2019. Inferences on plesiosaurian metabolic rate and vascular system from nutrient foramina in long bones. Society of Vertebrate Paleontology, 79th annual meeting, Abstracts of papers. Brisbane, QLD, Australia, p. 220.
- Woodward, H. N. 2019. *Maiasaura* (Dinosauria: Hadrosauridae) tibia osteohistology reveals non-annual cortical vascular rings in young of the year. *Frontiers in Earth Science* 7:50.
- Woodward, H. N., E. A. Freedman Fowler, J. O. Farlow, and J. R. Horner. 2015. *Maiasaura*, a model organism for extinct vertebrate population biology: a large sample statistical assessment of growth dynamics and survivorship. *Paleobiology* 41:503–527.